

Combining experimental and FEM approaches to determine the influence of workpiece temperature on fundamental variables in the machining process

ORTIZ-DE-ZARATE Gorka^{1,a*}, ARRIETA Iñaki M.^{1,b}, SORIANO Denis^{1,c},
ORUNA Ainara^{1,d}, SOLER Daniel^{1,e}, ARRAZOLA Pedro J.^{1,f}

¹Mondragon Unibertsitatea, Faculty of Engineering, Loramendi 4, Arrasate-Mondragón, 20500, Spain

^agortizdezarate@mondragon.edu, ^bimarrieta@mondragon.edu, ^cdsoriano@mondragon.edu,
^dainara.oruna@alumni.mondragon.edu, ^edsoler@mondragon.edu, ^fpjarrazola@mondragon.edu

Keywords: Hot Machining, FEM, Forces, Temperature, Orthogonal Cutting

Abstract. In machining it is common practice to use lubricants to enhance machinability, resulting in improved part quality and reduced tool wear. However, emerging efforts are centered on mitigating the environmental impact of conventional lubricants by embracing cryogenic (e.g., LN₂, CO₂) and hot machining (e.g., plasma/laser-assisted machining, resistance/induction heating) among others. However, few studies analyse in depth how the initial temperature of the workpiece affects the fundamental variables of the cutting process and consequently the machinability. In this scenario, this research aimed to analyse the influence of the workpiece temperature from 20°C to 500°C, on fundamental process variables, such as forces, chip morphology, Primary Shear Zone length, shear angle, and temperatures, when orthogonal cutting steel AISI 1045 combining experimental and Finite Element Method (FEM) approaches.

Introduction

Machining is one of the most complex manufacturing processes due to the high thermomechanical loads that occur during the generation of the new surface. For instance, it was observed that when machining steel AISI 1045 at a cutting speed of 300 m/min and a feed of 0.2 mm, strain rates of 10⁵ 1/s, strains of 4, and a heating rate of 10⁵ K/s are reached in the shearing zones [1]. Consequently, this behaviour generates thermomechanical loads that can produce: i) premature tool wear due to chemical reactivity between tool and workpiece materials promoted by the elevated temperatures, ii) subsurface microstructural alterations, and iii) surface defects in the workpiece, among others [2].

Intending to reduce the thermomechanical loads generated during machining the use of coolants and lubricants is a very widespread action to improve the quality of the component and reduce tool wear [3,4]. These substances, commonly oil-based fluids, are applied in the tool-chip interface, mainly to remove heat from the contact zone and reduce friction, which avoids early tool wear, and improves surface roughness [5]. However, these kinds of fluids are not only harmful to the environment but also toxic for the operator working on the machine, and some alternative methods, such as Minimum Quantity Lubrication (MQL), vegetable oil-based fluids, gaseous cooling or cryogenic cooling have raised in the last years [4,6]. Nonetheless, their cost is still high in comparison to conventional cutting fluids [4].

Another way to reduce the thermomechanical loads generated by the machining process is to heat the workpiece, also known as hot machining [7,8]. The most widely used methods according to literature to heat the workpiece are [7,8]: resistance [9], flame [10-12], plasma arc [13], laser-assisted [13], and induction [14-16]. Each of these heating methods has its advantages and disadvantages and is more suitable for one machining operation or another. For instance, laser,

plasma, and flame gas produce a very localised heat source, while resistance or induction can generate a more homogeneous heat throughout the workpiece.

Regarding the findings obtained in the field of manufacturing and production, many researchers have investigated optimizing the hot machining process and they have reported a reduction of forces or specific cutting coefficients, improvements in surface finishing, or increase in tool life when machining different metals [9-21]. Moon and Lee [13] observed that plasma-assisted milling yielded superior outcomes when applying to AISI 1045 and Inconel 718 workpieces, showing a decrease in cutting force and enhancement in surface integrity when compared to both laser-assisted and conventional (non-preheating) machining methods. The temperature of the workpiece was calculated by using heat transfer Finite Element Method (FEM) models. Unfortunately, controlling the initial temperature of the workpiece in those heating methods (plasma or laser assisted machining) is difficult.

Therefore, other alternatives, such as induction or resistant heating are more suitable for the precise control of the initial temperature of the workpiece. Baili et al. [14] studied the turning of the Ti-5553 alloy and found that by induction heating the workpieces to 750°C, the specific cutting forces were reduced by up to 34%, improving the surface finish as well as increasing the tool life. Choi and Lee [16] observed that induction assisted milling of AISI 1045 and Inconel 718, improves conventional machining in terms of forces, surface roughness, specific cutting energy, and tool life. Platt et al. [9] used resistance heating using cartridge heaters to increase the temperature of the workpiece (AISI M3:2 and AISI H11). They observed that as the temperature of the workpiece material increases, the yield strength and the hardness are reduced. This way it was possible to reduce the forces and the necessary power for the machining, increasing the process performance in terms of energy efficiency and tool life.

Hence, there are a few hot machining studies on AISI 1045 steel [13,16], and none of them are for turning. Additionally, most of them lack a more in-depth analysis of the influence of the initial temperature of the workpiece on scientific variables (forces, chip morphology, temperature, strain, strain rate, etc.), mainly because of the difficulty of measuring them experimentally.

To overcome that issue, a few studies are using numerical FEM modelling to gain a better understanding of the thermomechanical loads occurring in the hot machining process that are difficult to measure experimentally. The most relevant work was carried out by Xu et al. [22] and Parida and Maity [23]. Xu et al. [22] analyse the influence of the cutting speed, feed rate, depth of cut, and heating current (related to the workpiece temperature) on cutting forces when electric hot machining steel AISI 52100. Parida and Maity [23] studied the influence of nose radius (0.4, 0.8, and 1.2 mm) and initial workpiece temperature (20°C and 600°C) on forces, chip temperature, contact length, and chip morphology, using DEFORM FEM software for gas flame turning Inconel 718. Therefore, few studies develop FEM predictive models for hot machining applications, as also highlighted in the hot machining review paper of Pandey and Datta [1], and none of them are for steel AISI 1045.

To the best of the authors' knowledge, there are no studies in the literature that combine experimental tests and modelling to try to understand the influence of the initial workpiece temperature on fundamental variables when machining AISI 1045 steel. For this purpose, a new experimental setup was developed that enables the precise control of the initial workpiece temperature. Then, orthogonal cutting experimental tests were carried out at a wide range of initial workpiece temperatures (20-500°C) to analyse its influence on fundamental variables (forces, chip morphology, forces, chip morphology, Primary Shear Zone length, shear angle, and temperatures shear angle, and temperatures). Finally, a FEM model was developed for hot machining and validated against experimental outcomes, to understand the experimental results and gain knowledge about the thermomechanical loads variation with initial workpiece temperature.

Methodology

The experimental orthogonal cutting tests were carried out with a linear cutting setup on a Lagun GVC 1000-HS CNC milling machine that incorporated a Kistler 9139AA dynamometer to measure the forces (see Fig. 1). The workpiece material was steel AISI 1045 (155 Bhn), which was machined at constant cutting speed (30 m/min) and feed (0.2 mm) in dry conditions.

The initial temperature of the workpiece was varied between room temperature and 500°C (20, 300, 350, 400, 450 and 500°C). Thermoelectric resistors were used to increase the temperature of the workpiece in a controlled manner up to the target temperature. For this purpose, a control system was developed that incorporates a thermocouple clamped to the workpiece to ensure its temperature before the machining process. Additional thermocouples were also incorporated in preliminary tests in different areas of the workpiece (lateral sides, and surface to be machined) to analyse the homogeneity of the temperature across the workpiece for all the temperatures analysed (20-500°C). The difference between the values of the three thermocouples was less than 10°C. Therefore, although there may be a temperature gradient within the cut area due to the interaction of the thin workpiece with the environment, its effect does not seem to be very significant.

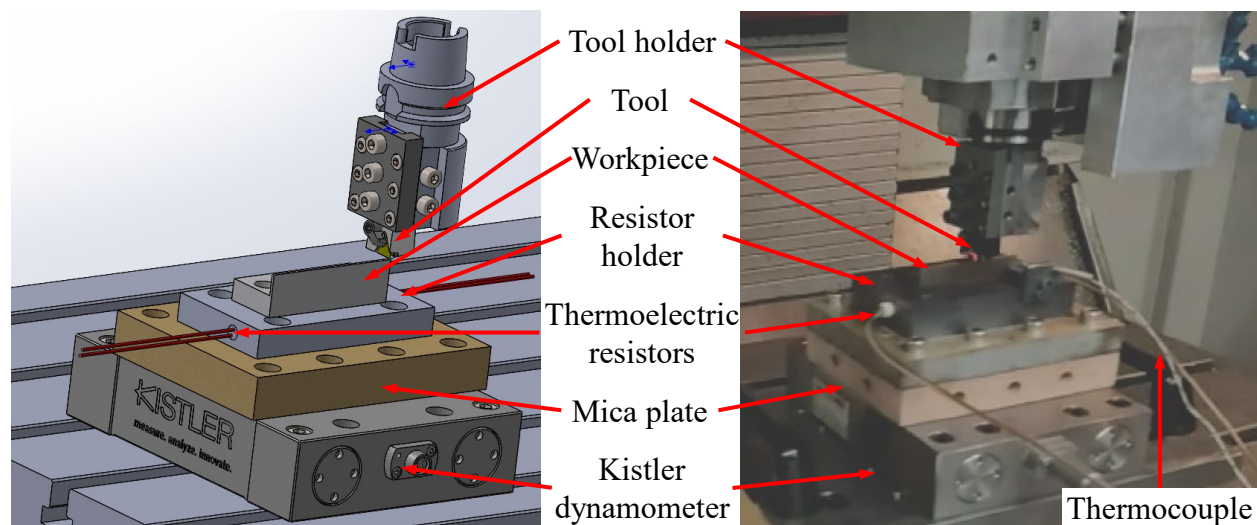


Fig. 1. Experimental setup for hot machining tests.

Furthermore, a Finite Element Method (FEM) model was created and validated for the prediction of fundamental variables (forces, chip morphology, temperatures, etc.). This model aimed to enhance understanding of the thermomechanical loads generated during the cutting process and study how they are affected by the initial workpiece temperature. Machining simulations were carried out using AdvantEdge™-2D V8.0, a specialized commercial finite element software for machining applications. The software employs a coupled thermo-elastoplastic Lagrangian code with continuous remeshing and adaptive meshing to avoid mesh distortion.

A 2D orthogonal cutting plane strain model was developed. The applied boundary conditions were categorized into thermal and mechanical. Fig. 2 illustrates all the boundary conditions that were implemented in the model. For the mechanical boundaries, the tool was fixed in two directions (X and Y), while the workpiece moved along the X direction at the cutting speed, and its displacement in the Y direction was restricted at the same nodes. Regarding the thermal boundary conditions, the outer counter of the workpiece and the rake and relief tool faces were treated as adiabatic. On the other hand, the bottom and top faces of the insert were designated as isothermal surfaces. Furthermore, conduction at the tool-chip interface was allowed. The initial temperature of the workpiece was also applied to the model, as in the experimental tests.

To achieve accurate results, the simulation employed a minimum element size of 5 μm , as illustrated in Fig. 2. Consequently, with a 4-core parallel processing setup, each simulation required approximately one hour.

The material properties of the tool and workpiece were obtained from the extensive library of the software. Nonetheless, the nominal hardness of the workpiece material of the software database is 200 Bhn, which is significantly higher than the one of the experimental workpiece material (155 Bhn). Therefore, the hardness of the workpiece material was changed in the software to match the experimental one. The software adjusted the material properties and the results obtained were closer to reality. Unfortunately, the software does not give any further information on how this adjustment is made.

The chosen friction law for the tool-chip contact was a sticking-sliding model [24]. This model was initially validated through the Split Tool methodology [25,26] and more recently supported by the Partially Restricted Contact Length Tools (PRCLT) approach [27], establishing as the most representative model for machining applications. A friction coefficient of 1 was specified based on the findings of these research works, which consistently concluded that it is the most suitable value for machining [25-27].

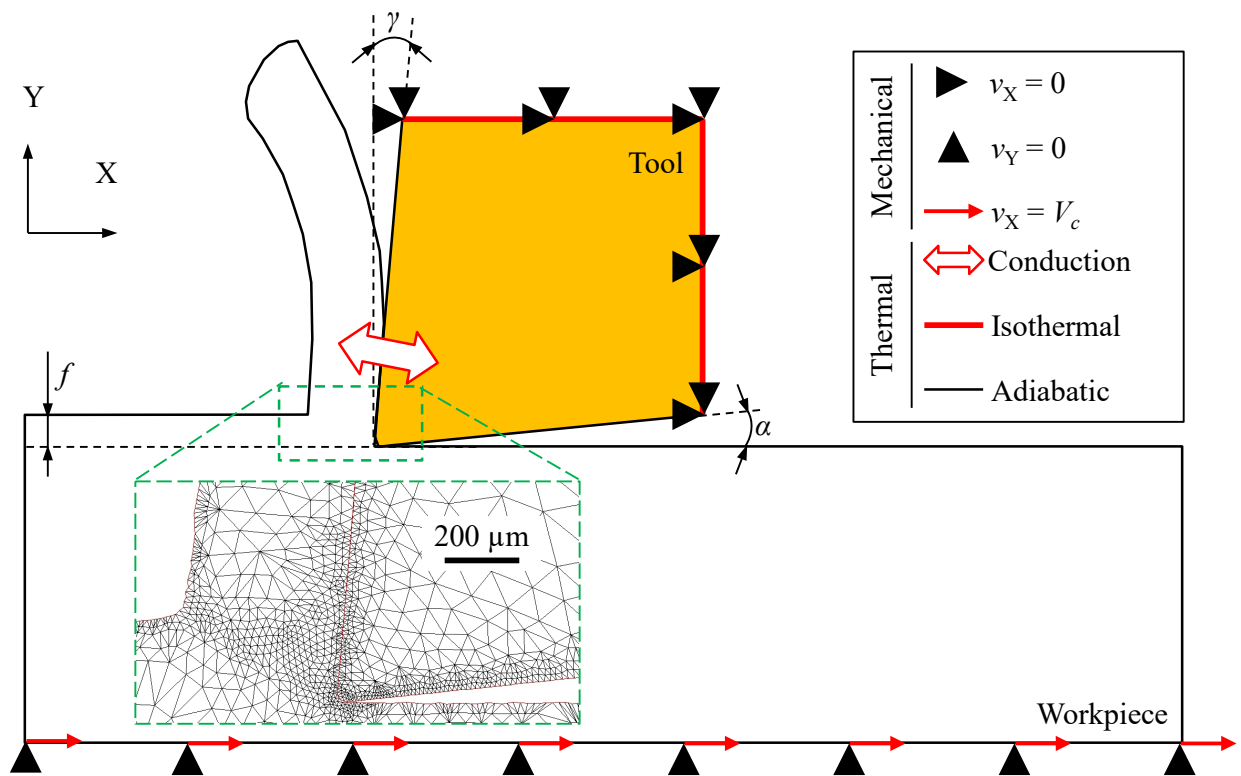


Fig. 2. Boundary conditions and mesh size of the orthogonal cutting FEM model.

The micro-geometry of the insert was assessed using an Alicona IFG4 optical profilometer. The configuration used consisted of a 10x polarised lens with a ring light to improve the quality of the profile acquisition. The vertical resolution was 1.5 μm , and the lateral resolution was 2.3 μm . The average cutting edge radius measured was $25 \pm 5 \mu\text{m}$. The rake (γ) and relief (α) angles of the inserts were 0° and 10° respectively, which were finally 6° and 4° respectively when the insert was positioned in the toolholder.

Results and discussion

Fig. 3 shows the cutting and feed forces (F_c and F_f), per unit of the depth of cut, obtained from the FEM model and experimentally. The FEM model accurately predicted the experimental trends and quantitative values. In the cutting forces, the average relative error was 8% and the maximum was

17% (for the initial workpiece temperature of 20°C). The overprediction of the cutting force at room temperature seems to be related to the flow stress model. This was obtained from the software database without being self-characterized, and there may be variations between the properties of the material used in the experimental tests and the one used to develop the flow stress model of the database. The feed forces were systematically overpredicted with an average relative error of 16% and a maximum of 22% (for the initial workpiece temperature of 450°C).

Regarding the influence of the initial temperature of the workpiece, it can be observed that the forces decrease when increasing the initial temperature from 20°C to 300°C. Then, above 300°C they remain constant, which was not initially expected, as the thermal softening in literature is more evident above 300-400°C than from 20°C to 300°C [28].

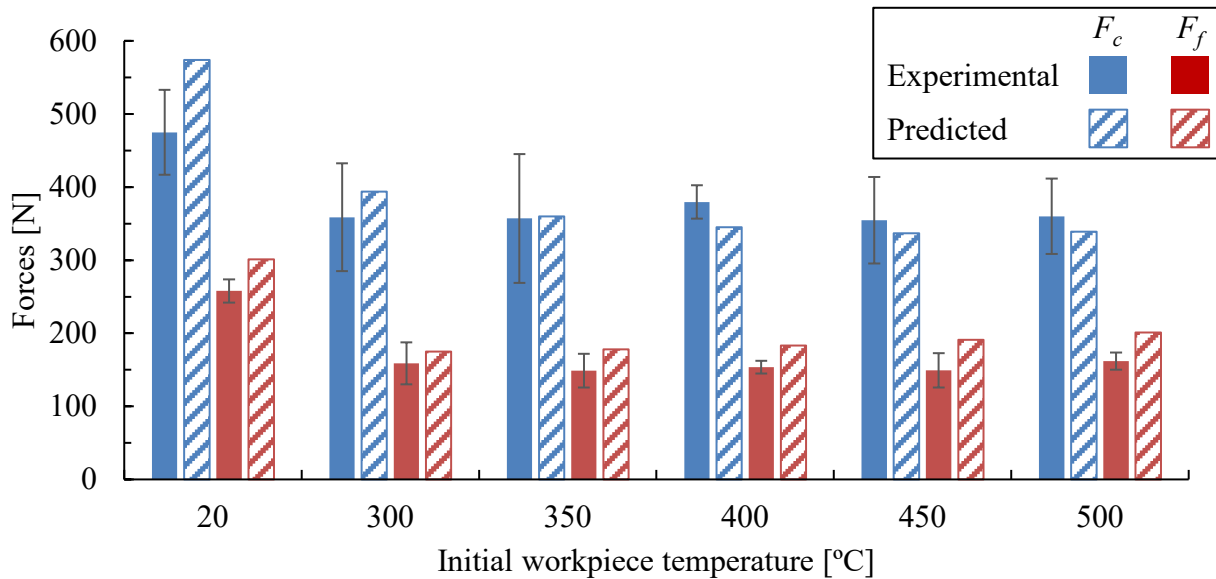


Fig. 3. Experimental and predicted forces.

There were also unexpected trends in the chip morphology (see Fig. 4), as the chip thickness changed non-linearly with the initial workpiece temperature. The chip thickness is reduced from 20°C to 350-400°C and then increases significantly from this temperature onwards. The trends observed experimentally were accurately predicted by the FEM model for all the analysed cutting conditions with an average relative error of 6% and a maximum of 14% for the initial workpiece temperature of 300°C. A continuous chip was obtained for all the simulations and experimentally.

To gain further insight into the reasons for the changing trends in forces and chip thickness with initial workpiece temperature, the shear angles (ϕ) and the Primary Shear Zone (PSZ) length were extracted from the simulations (see Fig. 4). As can be observed, the influence of the initial workpiece temperature on the chip thickness is fully related to the shear angle. The increase of the shear angle up to approximately the initial workpiece temperature of 350-400°C leads to a reduction of the chip thickness, while from that temperature onwards the shear angle decreases and consequently the chip thickness increases. In addition, an increase in chip thickness or reduction of the shear angle means a longer PSZ length, which in turn leads to increased forces, as long as the flow stress of the material in the PSZ is constant. For the flow stress to be constant, the variables affecting it (strain, strain rate, and temperature) must be constant.

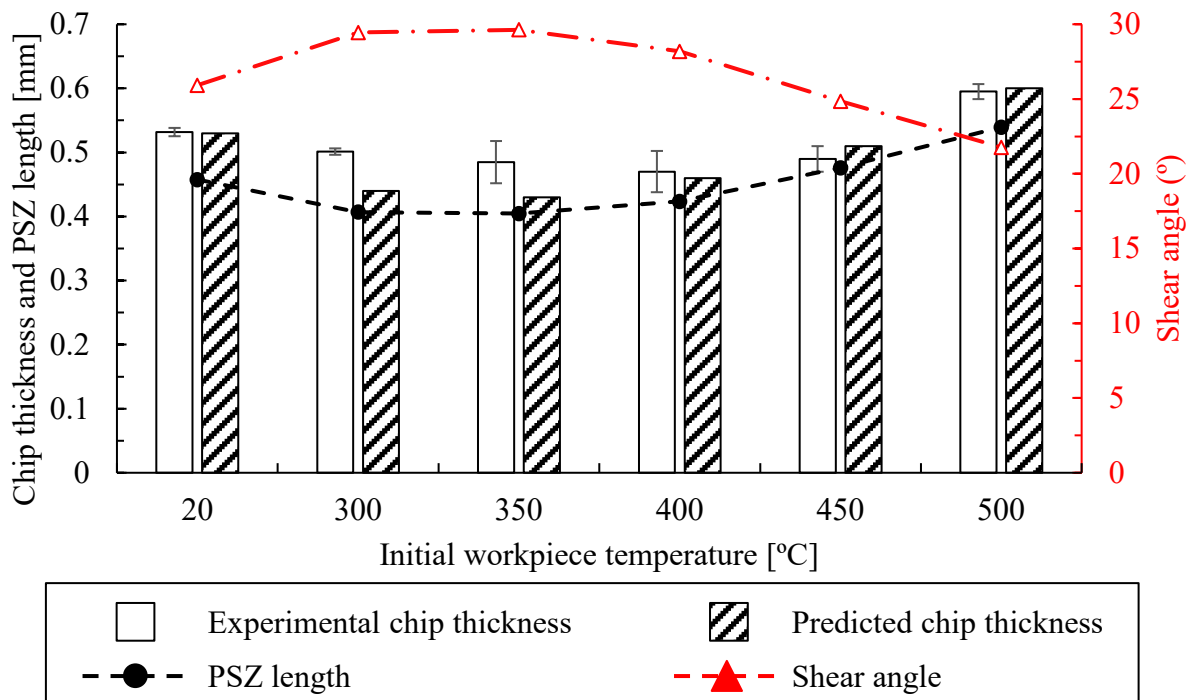


Fig. 4. Experimental and predicted chip thickness, shear angle, and Primary Shear Zone (PSZ) length.

Therefore, to analyse the flow stress behaviour in the PSZ the strain, strain rate, and temperature were extracted. 20 points were measured along the PSZ from each simulation (see Fig. 5). As can be seen, only the temperature is affected by the initial workpiece temperature, while the strain and strain rate are constant. Hence, it seems that there is a trade-off between the increase of the temperature in the PSZ with the increase of the length of the shear zone at temperatures above 300°C which keeps the forces almost constant. In addition, it should be noted that it was reported in the literature coupling between temperature and strain rate in AISI 1045 (higher strain rate hardening at higher temperatures) [28]. Therefore, there may be additional reasons related to material properties that could explain this phenomenon.

Therefore, the combination of the FEM simulation with the experimental tests has allowed to analyse how the initial temperature of the workpiece influences both the forces and the chip morphology and how they are affected by the scientific variables of the PSZ (shear angle, PSZ length, strain, strain rate and temperature).

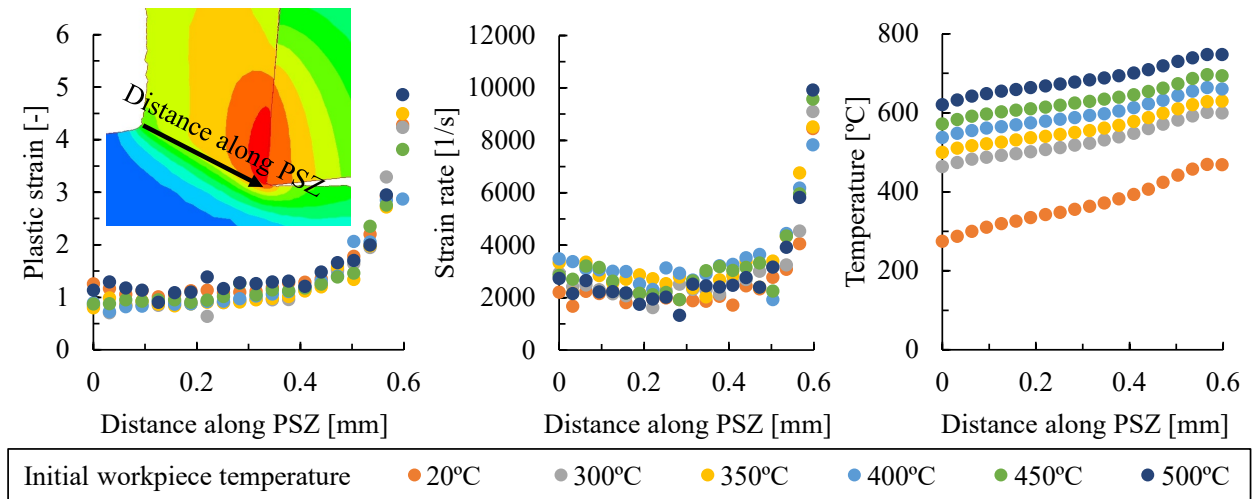


Fig. 5. Plastic strain, strain rate, and temperature along the Primary Shear Zone (PSZ).

After validation of the FEM model, the maximum tool temperature obtained for each initial temperature of the workpiece was extracted from the FEM model when the thermal steady state was reached. Fig. 6 shows: i) the maximum tool temperature, ii) the average PSZ temperature obtained from the data of Fig. 5, iii) the difference between the maximum tool temperature and the initial workpiece temperature, and iv) the difference between the maximum tool temperature and the average PSZ temperature. As can be seen in all cases the temperature change in the cutting zone is linearly proportional to the initial workpiece temperature.

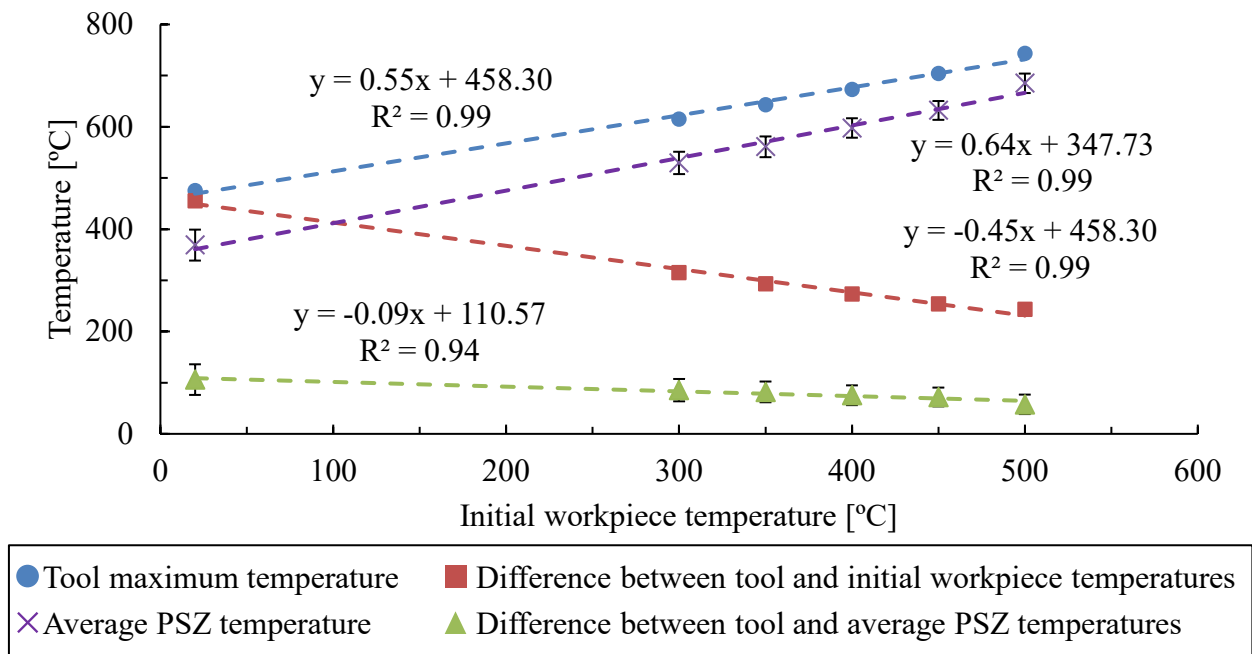


Fig. 6. Predicted temperatures.

In addition, it was observed that the difference between the initial workpiece temperature and the maximum tool temperature, is not constant. For instance, if the initial workpiece temperature is 20°C the maximum tool temperature reaches 475°C, resulting in a difference of 455°C. However, if the workpiece temperature is raised to 500°C, the tool temperature reaches 745°C giving a difference of only 245°C. On the contrary, the difference between the maximum tool temperature and the PSZ temperature remains almost constant, with a slight decrease, as the initial workpiece temperature is increased.

This means that an increase in the initial workpiece temperature does not mean an increase of the same magnitude in the maximum tool temperature, and this increase has a minimal effect on the PSZ temperature. This implies that wear can be kept low by selecting appropriate initial workpiece temperatures that allow reduced forces without resulting in increased tool wear due to an excessive increase in tool temperature.

Summary and conclusions

The influence of the initial workpiece temperature on fundamental variables (forces, chip morphology, shear angle, Primary Shear Zone length, strain, strain rate, and temperature) was investigated through a combination of experimental and Finite Element Method (FEM) approaches. The FEM model demonstrated precise predictions of cutting and feed forces, exhibiting an average relative error of 8% and 16%, respectively. Additionally, it accurately predicted chip thickness with a minimal error of 6%.

In the force analysis, it was observed that the forces were reduced as the initial workpiece temperature was increased from 20°C to 300°C. However, from 300°C up to 500°C, the forces remained constant. Analysing the Primary Shear Zone (PSZ), it was observed that the non-variation of the forces could come from the non-linear change of the shear angle and PSZ length together with the variation of the workpiece material properties (flow stress) in this zone. It was also found a correlation between the initial workpiece temperature and chip thickness, which was also related to the non-linear behaviour of the shear angle and PSZ length.

In addition, it was observed that a rise in the initial workpiece temperature does not proportionally increase the maximum tool temperature. Consequently, by choosing suitable initial workpiece temperatures that enable reduced forces without causing an excessive elevation in tool temperature, tool wear can be effectively minimized.

Taking all into account, hot machining seems to be a good alternative to reduce machining forces as long as there is a detailed knowledge of the influence of the temperature on the material properties (thermal softening, coupling between temperature and strain rate hardening, etc.). Not having sufficient knowledge of material behaviour can lead to: i) unnecessary energy waste by increasing the initial temperature of the workpiece to values that are not beneficial (e.g. going from 300°C to 500°C when machining AISI 1045), and ii) increasing the tool temperature excessively which could promote tool wear.

Acknowledgments

The authors hereby thank the projects SURFNANOCUT (RTI2018-095463-B-C21 and RTI2018-095463-B-C22), and TAILORSURF (PID2022-139655OB-I00).

References

- [1] P. J. Arrazola, F. Meslin, F. Le Maitre, S. Marya, Material flow stress sensitivity analysis in numerical cutting modeling, in AIP Conference Proceedings. 712/1 (2004) 1408–1413. <https://doi.org/10.1063/1.1766726>
- [2] Z. Liao, A. la Monaca, J. Murray, A. Speidel, D. Ushmaev, A. Clare, D. Axinte, R. M'Saoubi, Surface integrity in metal machining-Part I: Fundamentals of surface characteristics and formation mechanisms, International Journal of Machine Tools and Manufacture. 162 (2021) 103687. <https://doi.org/10.1016/j.ijmachtools.2020.103687>
- [3] G. W. A. Kui, S. Islam, M. M. Reddy, N. Khandoker, V. L. C. Chen, Recent progress and evolution of coolant usages in conventional machining methods: a comprehensive review, International Journal of Advanced Manufacturing Technology. 119/1-2 (2022) 3-40. <https://doi.org/10.1007/s00170-021-08182-0>

- [4] E. Benedicto, D. Carou, E. M. Rubio, Technical, Economic and Environmental Review of the Lubrication/Cooling Systems Used in Machining Processes, *Procedia engineering*. 184 (2017) 99-116. <https://doi.org/10.1016/j.proeng.2017.04.075>
- [5] S. H. Musavi, B. Davoodi, B. Eskandari, Evaluation of surface roughness and optimization of cutting parameters in turning of AA2024 alloy under different cooling-lubrication conditions using RSM method, *Journal of Central South University*. 27 (2020) 1714-1728. <https://doi.org/10.1007/s11771-020-4402-2>
- [6] S. Pervaiz, I. Deiab, A. Rashid, M. Nicolescu, Minimal quantity cooling lubrication in turning of Ti6Al4V : Influence on surface roughness, cutting force and tool wear, *Proceedings of the Institution of Mechanical Engineers, Part B: Journal of Engineering Manufacture*. 231/9 (2017) 1542-1558. <https://doi.org/10.1177/095440541559994>
- [7] K. Pandey, S. Datta, Hot machining of difficult-to-cut materials : A review, *Materials Today: Proceedings*. 44 (2021) 2710-2715. <https://doi.org/10.1016/j.matpr.2020.12.687>
- [8] K. A. Mohammed, J. J. Abdulhameed, E. S. Al-Ameen, The effectiveness of hot machining process for the machinability of hard to cut materials: A review, *IOP Conference Series: Materials Science and Engineering*. 870/1 (2020) 012140. <https://doi.org/10.1088/1757-899X/870/1/012140>
- [9] T. Platt, A. Meijer, D. Biermann, Conduction-based thermally assisted micromilling process for cutting difficult-to-machine materials, *Journal of Manufacturing and Materials Processing*. 4/2 (2020) 34. <https://doi.org/10.3390/jmmp4020034>
- [10] N. M. Kamdar, P. V. K. Patel, Experimental Investigation of Machining Parameters of EN 36 Steel using Tungsten Carbide Cutting Tool during Hot Machining, *International Journal of Engineering Research and Applications*. 2 (2012) 1833-1838.
- [11] N. Tosun, L. Ozler, Optimisation for hot turning operations with multiple performance characteristics, *International Journal of Advanced Manufacturing Technology*. 23 (2004) 777-782. <https://doi.org/10.1007/s00170-003-1672-4>
- [12] R. D. Rajopadhye, M. T. Telsang, N. S. Dhole, Experimental Setup for Hot Machining Process to Increase Tool Life with Torch Flame, *Second international conference on emerging trends in engineering (SICETE)*. (2009) 58-62.
- [13] S. H. Moon, C. M. Lee, A study on the machining characteristics using plasma assisted machining of AISI 1045 steel and Inconel 718, *International Journal of Mechanical Sciences*. 142 (2018) 595-602. <https://doi.org/10.1016/j.ijmecsci.2018.05.020>
- [14] M. Baili, V. Wagner, G. Desein, J. Sallaberry, D. Lallement, An experimental investigation of hot machining with induction to improve Ti-5553 machinability, *Applied mechanics and Materials*. 62 (2011) 67-76. <https://doi.org/10.4028/www.scientific.net/AMM.62.67>
- [15] S. Ranganathan, T. Senthilvelan, Multi-response optimization of machining parameters in hot turning using grey analysis, *The International Journal of Advanced Manufacturing Technology*. 56 (2011) 455-462. <https://doi.org/10.1007/s00170-011-3198-5>
- [16] Y. H. Choi, C. M. Lee, A study on the machining characteristics of AISI 1045 steel and inconel 718 with circular cone shape in induction assisted machining, *Journal of Manufacturing Processes*. 34 (2018) 463-476. <https://doi.org/10.1016/j.jmapro.2018.06.023>
- [17] O. Çakır, E. Altan, Hot machining of high manganese steel: a review, *Trends in the development of machinery and associated technology*. (2008) 105-108.

- [18] N. R. Modh, G. D. Mistry, K. B. Rathod, An experimental investigation to optimize the process parameters of AISI 52100 steel in hot machining, *International Journal of Engineering Research and Applications*. 1/3 (2011) 483-489.
- [19] A. K. Kumar, P. Venkataramaiah, Optimization of Process parameters in hot machining of Inconel 718 alloy using FEM, *International Journal of Applied Engineering Research*. 13/5 (2018) 2158-2162.
- [20] S. K. Thandra, S. K. Choudhury, Effect of cutting parameters on cutting force, surface finish and tool wear in hot machining, *International Journal of Machining and Machinability of Materials*. 7/3-4 (2010) 260-283. <https://doi.org/10.1504/IJMMM.2010.03307>
- [21] A. K. Parida, K. Maity, Hot machining of Ti – 6Al – 4V : FE analysis and experimental validation, *Sādhanā*. 44 (2019) 1-6. <https://doi.org/10.1007/s12046-019-1127-8>
- [22] W. Xu, X. Liu, J. Sun, L. Zhang, Finite element simulation and experimental research on electric hot machining, *International Journal of Advanced Manufacturing Technology*. 66 (2013) 407-415. <https://doi.org/10.1007/s00170-012-4335-5>
- [23] A. K. Parida, K. Maity, Effect of nose radius on forces, and process parameters in hot machining of Inconel 718 using finite element analysis, *Engineering Science and Technology, an International Journal*. 20/2 (2017) 687-693. <https://doi.org/10.1016/j.jestch.2016.10.006>
- [24] N. N. Zorev, Inter-relationship between shear processes occurring along tool face and shear plane in metal cutting, *International research in production engineering*. 49 (1963) 142-152.
- [25] S. Kato, K. Yamaguchi, M. Yamada, Stress distribution at the interface between tool and chip in machining, *Journal of Manufacturing Science and Engineering, Transactions of the ASME*. 94/2 (1972) 693-689. <https://doi.org/10.1115/1.3428229>
- [26] K. Maekawa, T. Kitagawa, T. H. C. Childs, Friction characteristics at tool-chip interface in steel machining, *Tribology Series*. 32 (1997) 559–567. [https://doi.org/10.1016/S0167-8922\(08\)70482-6](https://doi.org/10.1016/S0167-8922(08)70482-6)
- [27] G. Ortiz de Zarate, A. Madariaga, P. J. Arrazola, T. H. C. Childs, A novel methodology to characterize tool-chip contact in metal cutting using partially restricted contact length tools, *CIRP Annals*. 70/1 (2021) 61-64. <https://doi.org/10.1016/j.cirp.2021.03.002>
- [28] M. Saez-de-Buruaga, P. Aristimuño, D. Soler, E. D'Eramo, A. Roth, P. J. Arrazola, Microstructure based flow stress model to predict machinability in ferrite–pearlite steels, *CIRP Annals*. 68/1 (2019) 49-52. <https://doi.org/10.1016/j.cirp.2019.03.013>